

Optimal Eigenvalue and Asymptotic Large Time Approximations Using the Moving Finite Element Method

P.K. Jimack

School of Computer Studies

University of Leeds

Leeds LS2 9JT, UK

Key words. Moving Finite Elements, Eigenvalue Problems, Best Free Knot Approximations

AMS(MOS) subject classification. 65M60

Abstract

The Moving Finite Element method for the solution of time-dependent partial differential equations is a numerical solution scheme which allows the automatic adaption of the finite element approximation space with time, through the use of mesh relocation (r -refinement). This paper analyses the asymptotic behaviour of the method for large times when it is applied to the solution of a class of self-adjoint parabolic equations in an arbitrary number of space dimensions. It is shown that asymptotically the method will produce solutions which converge to a fixed mesh and it is proved that such a mesh allows an optimal approximation of the slowest decaying eigenvalue and eigenfunction for the problem. Hence it is demonstrated that the Moving Finite Element method can yield an optimal solution to such parabolic problems for large times.

1 Introduction

The Moving Finite Element (MFE) method for the solution of time-dependent partial differential equations, is a spatial semi-discretization in which the finite element mesh itself is an unknown of the problem, as well as the representation of the solution on that mesh ([5, 11, 12]). As time proceeds, the mesh evolves, so that it should always permit an accurate representation of the solution.

Due to the highly nonlinear nature of this algorithm, for which the finite element subspace being used is itself time-dependent, it is quite difficult to analyze many of the features that are well understood for more conventional finite element techniques. Nevertheless, in [2] it is shown that the

Moving Finite Element mesh is able to follow characteristics when applied to hyperbolic problems and in [7] it is shown that, for certain parabolic p.d.e.'s, the MFE mesh evolves so as to allow an optimum approximation of the steady solution of the differential equation over all free-knot spline representations. This last result, which was first suggested by Miller ([12]), only yields information about steady solutions however and tells us nothing about how they may evolve. In this paper we take a step towards analyzing the temporal properties of the MFE solutions to problems of a parabolic nature. We do this through the study of a simple model problem, and, in the first instance, by limiting our investigation to the asymptotic behaviour for large times.

Consider the equation

$$\frac{\partial u}{\partial t}(\underline{x}, t) = \frac{\partial}{\partial x_i}(p_{ij}(\underline{x})\frac{\partial u}{\partial x_j}(\underline{x}, t)) - q(\underline{x})u(\underline{x}, t) \quad \forall \underline{x} \in \Omega \subseteq \mathbb{R}^D \text{ and } t \in (0, T], \quad (1.1)$$

where D is any positive integer (but is typically 1, 2 or 3), $T \gg 0$ and the summation convention for repeated suffices has been applied. Also, we assume that the matrix $P(\underline{x})$, whose entries are $p_{ij}(\underline{x})$, is symmetric and positive definite and that

$$\text{each } p_{ij}(\underline{x}) \in C^{1,\alpha}(\Omega), \quad q \in C^{0,\alpha}(\Omega), \quad \text{and} \quad q \geq 0$$

for all $\underline{x} \in \Omega$ (where $\alpha \in (0, 1)$). Finally we will assume for simplicity that the boundary $\partial\Omega$ is piecewise affine, convex and satisfies the homogeneous Dirichlet boundary condition

$$u(\underline{x}, t)|_{\partial\Omega} = 0 \quad \forall t \in (0, T]. \quad (1.2)$$

Although this problem has the unique steady solution $u \equiv 0$, given any initial condition, $u(\underline{x}, 0)$, which is not identically zero on Ω , $u(\underline{x}, t)$ will never reach this steady state for any finite T . To study the asymptotic behaviour of the solution we consider the closely related eigenvalue problem

$$\frac{\partial}{\partial x_i}(p_{ij}(\underline{x})\frac{\partial u}{\partial x_j}(\underline{x})) - q(\underline{x})u(\underline{x}) = -\lambda u(\underline{x}); \quad u(\underline{x})|_{\partial\Omega} = 0, \quad (1.3)$$

since if $\hat{u}(\underline{x})$ is a solution of this problem then $u(\underline{x}, t) = e^{-\lambda t}\hat{u}(\underline{x})$ is a solution of (1.1). In particular, the solution of (1.3) with the smallest eigenvalue, λ_1 say, is of special interest since this represents the slowest decaying mode in the solution of the original problem (1.1). (Note that the above restrictions on P and q ensure that all of the eigenvalues, λ , are positive.)

The theory for the standard Galerkin finite element solution of (1.1) and (1.3) is well known (see [17] for example). In particular, all of the eigenvalues of (1.3) are approximated from above by the finite element method. In this paper we will make use of this fact to prove that the Moving Finite Element method allows an optimum approximation to the fundamental eigenvalue λ_1 over all

variations in the finite element mesh. This in turn implies that the MFE solution of (1.1) is also optimal for large T in the sense that it gives an optimal approximation to the fundamental mode in terms of its rate of decay, a feature that was hypothesised in [6].

2 The Moving Finite Element Method

In this section we give a brief outline of the Moving Finite Element method and how it may be used to solve the linear evolution equation (1.1) along with its associated boundary conditions (1.2). We develop all of the theory in this paper for an arbitrary number of dimensions, D , although readers may prefer to concentrate on the case $D = 2$, for example, where the finite elements are triangular and the domain is polygonal (the case $D = 1$ simplifies things even further of course). Also, further details of the method, and its implementations, may be found in [2, 5, 18] for example.

In order to proceed it will be helpful to introduce some notation. It is possible to discretize Ω into a set of non-overlapping simplexes which can be uniquely specified as a mesh $\mathcal{M} = (\underline{s}, \mathcal{C})$, where

$$\underline{s} = (\underline{s}_1, \dots, \underline{s}_N, \underline{s}_{N+1}, \dots, \underline{s}_{N+B}) \quad (2.1)$$

is an ordered set of the position vectors of the vertices of the mesh (N interior points and B points on the boundary), and \mathcal{C} is a list of all of the edges. The MFE method seeks to approximate $u(\underline{x}, t)$, the solution of (1.1), by a time-dependent piecewise linear function, u^h say, defined on a mesh of simplexes $\mathcal{M}(t) = (\underline{s}(t), \mathcal{C})$ covering the spatial domain Ω . As has been indicated, this mesh is allowed to deform smoothly in time by allowing the positions of the internal knot points, $\underline{s}_1(t), \dots, \underline{s}_N(t)$, to be time-dependent. Their connectivity \mathcal{C} remains fixed however.

Because \mathcal{C} is kept fixed throughout we will generally refer to a mesh $\mathcal{M}(t) = (\underline{s}(t), \mathcal{C})$ only by the ordered set $\underline{s}(t)$ for notational convenience. Given this, and using (1.2), we can write our approximation u^h in the form

$$u^h(\underline{x}, t) = \sum_{m=1}^N a_m(t) \alpha_m(\underline{x}, \underline{s}(t)) , \quad (2.2)$$

where α_m is the usual continuous piecewise linear ‘‘hat’’ basis function on the mesh $\underline{s}(t)$:

$$\alpha_m(\underline{s}_n(t), \underline{s}(t)) = \delta_{mn} , \quad m = 1, \dots, N ; \quad n = 1, \dots, N + B .$$

In order to determine this approximation to $u(\underline{x}, t)$ we need to find values for the unknowns $a_1(t), \underline{s}_1(t), \dots, a_N(t), \underline{s}_N(t)$. The Moving Finite Element method does this by producing a weak or variational form of (1.1) for which the trial solution u^h takes the form of (2.2) and the test space is

the space in which the function $\frac{\partial u^h}{\partial t}$ lies at each instant in time. In order to determine this space we differentiate (2.2) with respect to time to give

$$\frac{\partial u^h}{\partial t} = \frac{\partial}{\partial t} \sum_{m=1}^N a_m(t) \alpha_m(\underline{x}, \underline{s}(t)) = \sum_{m=1}^N \dot{a}_m \alpha_m + \sum_{m=1}^N a_m \frac{\partial \alpha_m}{\partial \underline{s}} \cdot \frac{d\underline{s}}{dt} \quad (2.3)$$

$$= \sum_{m=1}^N \dot{a}_m \alpha_m + \frac{\partial u^h}{\partial \underline{s}} \cdot \frac{d\underline{s}}{dt} = \sum_{m=1}^N \dot{a}_m \alpha_m + \sum_{m=1}^N \dot{\underline{s}}_m \cdot \frac{\partial u^h}{\partial \underline{s}_m} = \sum_{m=1}^N (\dot{a}_m \alpha_m + \dot{\underline{s}}_m \cdot \underline{\beta}_m), \quad (2.4)$$

where $\underline{\beta}_m = \frac{\partial u^h}{\partial \underline{s}_m} = (\frac{\partial u^h}{\partial s_{m1}}, \dots, \frac{\partial u^h}{\partial s_{mD}})^T$ and the dot above a variable denotes differentiation with respect to time. Hence the Moving Finite Element method takes a weak form of (1.1) for which the test space is the space spanned by

$$\{\alpha_1, \beta_{11}, \dots, \beta_{1D}; \dots; \alpha_N, \beta_{N1}, \dots, \beta_{ND}\}.$$

The most straightforward weak form of this type is the simple generalization of the Galerkin method given formally by the differential system

$$\left\langle \sum_{m=1}^N (\dot{a}_m \alpha_m + \dot{\underline{s}}_m \cdot \underline{\beta}_m), \alpha_n \right\rangle = \left\langle \frac{\partial}{\partial x_i} (p_{ij} \frac{\partial u^h}{\partial x_j}) - q u^h, \alpha_n \right\rangle \quad (2.5)$$

and

$$\left\langle \sum_{m=1}^N (\dot{a}_m \alpha_m + \dot{\underline{s}}_m \cdot \underline{\beta}_m), \beta_{ne} \right\rangle = \left\langle \frac{\partial}{\partial x_i} (p_{ij} \frac{\partial u^h}{\partial x_j}) - q u^h, \beta_{ne} \right\rangle \quad (2.6)$$

for the unknowns $a_1(t), \underline{s}_1(t), \dots, a_N(t), \underline{s}_N(t)$, with $n = 1, \dots, N$ and $e = 1, \dots, D$. In the above notation $\langle \cdot, \cdot \rangle$ represents the usual L^2 inner product on Ω .

Lemma 2.1

$$\frac{\partial \alpha_\ell}{\partial s_{md}} = -\alpha_m \frac{\partial \alpha_\ell}{\partial x_d} \quad \text{for } \ell = 1, \dots, N; \quad d = 1, \dots, D, \quad (2.7)$$

hence

$$\beta_{md} = \frac{\partial u^h}{\partial s_{md}} = -\alpha_m \frac{\partial u^h}{\partial x_d} \quad \text{for } d = 1, \dots, D, \quad \text{and so } \underline{\beta}_m = \frac{\partial u^h}{\partial \underline{s}_m} = -\alpha_m \underline{\nabla} u^h. \quad (2.8)$$

Proof See [8].

In view of the above lemma, it should be noted that the second of these sets of equations is not properly defined for a piecewise linear function $u^h(\underline{x}, t)$, even in a distributional sense. To overcome this difficulty it is necessary to express these equations in a formally equivalent form which is well-defined for such functions u^h :

$$\sum_{m=1}^N \int_{\Omega} \alpha_m \alpha_n \, d\underline{x} \, \dot{a}_m + \sum_{m=1}^N \sum_{d=1}^D \int_{\Omega} \beta_{md} \alpha_n \, d\underline{x} \, \dot{s}_{md} = - \int_{\Omega} q u^h \alpha_n \, d\underline{x} - \int_{\Omega} p_{ij} \frac{\partial u^h}{\partial x_j} \frac{\partial \alpha_n}{\partial x_i} \, d\underline{x} \quad (2.9)$$

and

$$\begin{aligned} \sum_{m=1}^N \int_{\Omega} \alpha_m \beta_{ne} d\underline{x} \dot{a}_m + \sum_{m=1}^N \sum_{d=1}^D \int_{\Omega} \beta_{md} \beta_{ne} d\underline{x} \dot{s}_{md} = & - \int_{\Omega} q u^h \beta_{ne} d\underline{x} - \frac{1}{2} \int_{\Omega} \frac{\partial u^h}{\partial x_i} \frac{\partial u^h}{\partial x_j} \frac{\partial}{\partial x_e} (\alpha_n p_{ij}) d\underline{x} \\ & + \int_{\Omega} p_{ij} \frac{\partial u^h}{\partial x_j} \frac{\partial \alpha_n}{\partial x_i} \frac{\partial u^h}{\partial x_e} d\underline{x} \end{aligned} \quad (2.10)$$

for $n = 1, \dots, N$ and $e = 1, \dots, D$. See [7] for details.

The sets of equations (2.9) and (2.10) are referred to as the Moving Finite Element equations. They form a system of ordinary differential equations which may be written in the form

$$A(\underline{y}) \dot{\underline{y}} = \underline{g}(\underline{y}), \quad (2.11)$$

where

$$\underline{y} = (a_1, \dots, a_N; s_{11}, \dots, s_{1D}; \dots; s_{N1}, \dots, s_{ND})^T,$$

$$\underline{\alpha} = (\alpha_1, \dots, \alpha_N; \beta_{11}, \dots, \beta_{1D}; \dots; \beta_{N1}, \dots, \beta_{ND})^T,$$

$$A = \langle \underline{\alpha}, \underline{\alpha}^T \rangle$$

and \underline{g} is the vector of right-hand-sides. The matrix $A(\underline{y})$ will be referred to as the ‘‘MFE mass matrix’’. It should be noted that even though (1.1) is linear, the Moving Finite Element semi-discretization yields a non-linear system of differential equations (2.11). From a practical viewpoint this makes the method extremely uncompetitive for the adaptive solution of linear p.d.e.’s. In performing this analysis therefore, we are not advocating the use of such a sophisticated solution technique for such straightforward problems. The objective is to use test problems such as this as a key to gaining some insight into the nature and fundamental properties of the method.

Lemma 2.2 *The matrix $A(\underline{y})$ is positive semi-definite and is singular if and only if the functions in the ordered set $\underline{\alpha}$, defined above, form a linearly dependent set. Further, such a linear dependence can occur if and only if the MFE solution, u^h , has a directional derivative which is continuous at one or more of the knot points $\underline{s}_1, \dots, \underline{s}_N$.*

Proof See [19]. (The proof given is for the case $D = 2$ but generalizes to arbitrary dimensions.)

When the matrix $A(\underline{y})$ in this system is singular due to u^h having a continuous directional derivative at a knot point, the MFE solution will be described as ‘‘degenerate’’. Otherwise it will be said to be ‘‘non-degenerate’’, in which case $A(\underline{y})$ is strictly positive definite. The difficulties associated with degeneracy along with the possibility of the area of one or more of the elements in the mesh becoming non-positive as the knot points evolve are often cited as two of the major drawbacks of

the MFE method. One approach to overcoming these difficulties is to influence the nodal motion by using penalty terms in equations (2.9) and (2.10). This is the approach of Miller *et al*, [5, 11, 12], and Mueller and Carey [13] for example. However, much of the work of Baines *et al*, [1, 2, 3, 4, 9, 19], suggests that the use of such penalties may not always be necessary. Throughout this paper we analyze the method described above, without penalty terms. This may be justified not only by the fact that the method often works well without them, but also because gaining a clear understanding of underlying method will contribute to the understanding of its numerous variants (see [2]), and perhaps also lead to the derivation of new ones.

3 Large-Time Solutions of the Moving Finite Element Equations

In this section we demonstrate that the MFE method can produce optimal grids for the solution of eigenvalue problems of the form (1.3). Suppose we have a fixed mesh $\mathcal{M} = (\underline{s}, \mathcal{C})$, with \underline{s} as defined in the previous section, (2.1). Then we may define the subspace $S_0^h(\underline{s}) \subset H_0^1(\Omega)$ to consist of the piecewise linear functions on \underline{s} which vanish on the boundary (i.e. of the form given by (2.2)). It is well known (see [17] for example) that the Galerkin finite element approximations to the eigenfunctions, v_k , of equation (1.3) correspond to finding the stationary points of the Rayleigh quotient

$$R(v) = \frac{a(v, v)}{\langle v, v \rangle} = \frac{\int_{\Omega} (\frac{\partial v}{\partial x_i} p_{ij} \frac{\partial v}{\partial x_j} + qv^2) d\underline{x}}{\int_{\Omega} v^2 d\underline{x}} \quad (3.1)$$

in the finite element subspace $S_0^h(\underline{s})$. In particular, the minimizer, $v_1^h(\underline{s})$ say, gives an approximation to the principal eigenfunction in (1.3), v_1 say, and $R(v_1^h(\underline{s})) = \lambda_1^h(\underline{s})$, say, gives an approximation to the fundamental eigenvalue in (1.3), λ_1 . We will demonstrate below that applying the Moving Finite Element method to equation (1.1) can produce a finite element mesh, \underline{s}^* say, such that

$$|\lambda_1 - \lambda_1^h(\underline{s}^*)| \leq |\lambda_1 - \lambda_1^h(\underline{s})| \quad (3.2)$$

for all \underline{s} in some neighbourhood of \underline{s}^* . That is, the Moving Finite Element method can produce a (locally) optimal mesh for approximating the fundamental solution of equation (1.3) and hence for the large-time solution of (1.1) as well.

In order to prove this we first establish two intermediate results which are expressed as lemmas 3.1 and 3.2 below. The second of these will be of direct use to us, whilst the first (which is proved in [7]) is only necessary to break up the proof of lemma 3.2.

Lemma 3.1 *Consider a D -dimensional simplex with vertices at $\hat{\underline{x}}_0, \hat{\underline{x}}_1, \dots, \hat{\underline{x}}_D$ and measure $A_E(\hat{\underline{x}}) > 0$. Let $\tilde{\alpha}_R$ be the local linear basis function on this simplex such that*

$$\tilde{\alpha}_R(\hat{\underline{x}}_i) = \delta_{iR} \quad \text{for } i, R \in \{0, 1, \dots, d\}.$$

Then

$$\frac{\partial A_E}{\partial \hat{s}_{Re}} = \frac{\partial \tilde{\alpha}_R}{\partial x_e} A_E \quad \text{for } R \in \{0, 1, \dots, D\} \text{ and } e \in \{1, \dots, D\}.$$

Lemma 3.2 Let $\lambda_1^h(\underline{s})$ and $v_1^h(\underline{s})$ (with $\langle v_1^h(\underline{s}), v_1^h(\underline{s}) \rangle = 1$) be the Galerkin finite element approximations to the fundamental eigenvalue, λ_1 , and the normalized fundamental eigenfunction, v_1 , for equation (1.3), on a mesh with vertices \underline{s} . Then

$$\begin{aligned} \frac{\partial \lambda_1^h}{\partial s_{ne}} &= \int_{\Omega} \frac{\partial v_1^h}{\partial x_i} \frac{\partial}{\partial x_e} (\alpha_n p_{ij}) \frac{\partial v_1^h}{\partial x_j} d\underline{x} - 2 \int_{\Omega} \frac{\partial v_1^h}{\partial x_e} \frac{\partial \alpha_n}{\partial x_i} p_{ij} \frac{\partial v_1^h}{\partial x_j} d\underline{x} \\ &\quad - 2 \int_{\Omega} q \frac{\partial v_1^h}{\partial x_e} \alpha_n v_1^h d\underline{x} + 2\lambda_1^h \int_{\Omega} \frac{\partial v_1^h}{\partial x_e} \alpha_n v_1^h d\underline{x}, \end{aligned} \quad (3.3)$$

for $n = 1, \dots, N$ and $e = 1, \dots, D$ (using the summation convention (from 1 to D) on i and j).

Proof As $v_1^h(\underline{s}) \in S_0^h(\underline{s})$, we may express it in the form

$$v_1^h(\underline{s}) = \sum_{m=1}^N v_m^{(1)}(\underline{s}) \alpha_m(\underline{x}, \underline{s}) = v_m^{(1)} \alpha_m,$$

and since $\langle v_1^h(\underline{s}), v_1^h(\underline{s}) \rangle = 1$ we may observe that

$$1 = \int_{\Omega} (v_\ell^{(1)} \alpha_\ell)(v_m^{(1)} \alpha_m) d\underline{x} = v_\ell^{(1)} M_{\ell m} v_m^{(1)}, \quad (3.4)$$

where

$$M_{\ell m}(\underline{s}) = \int_{\Omega} \alpha_\ell(\underline{x}, \underline{s}) \alpha_m(\underline{x}, \underline{s}) d\underline{x}.$$

Also, the Galerkin finite element discretization of (1.3) implies that the relation

$$(\tilde{K}_{\ell m} + \tilde{M}_{\ell m} - \lambda_1^h M_{\ell m}) v_m^{(1)} = 0 \quad (3.5)$$

must be satisfied by $\lambda_1^h(\underline{s})$ and $v_1^h(\underline{s})$ for each $\ell \in \{1, \dots, N\}$, where

$$\tilde{K}_{\ell m}(\underline{s}) = \int_{\Omega} \frac{\partial \alpha_\ell}{\partial x_i}(\underline{x}, \underline{s}) p_{ij}(\underline{x}) \frac{\partial \alpha_m}{\partial x_j}(\underline{x}, \underline{s}) d\underline{x} \quad \text{and} \quad \tilde{M}_{\ell m}(\underline{s}) = \int_{\Omega} q(\underline{x}) \alpha_\ell(\underline{x}, \underline{s}) \alpha_m(\underline{x}, \underline{s}) d\underline{x}. \quad (3.6)$$

(Note that the repeated suffices i and j imply summation from 1 to D , whereas the repeated suffices ℓ and m imply summation from 1 to N .)

From equations (3.5) it easily follows that the relation

$$v_\ell^{(1)} (\tilde{K}_{\ell m} + \tilde{M}_{\ell m} - \lambda_1^h M_{\ell m}) v_m^{(1)} = 0 \quad (3.7)$$

must also be satisfied by $\lambda_1^h(\underline{s})$ and $v_1^h(\underline{s})$. Now, differentiating (3.7) with respect to s_{ne} (for any $n \in \{1, \dots, N\}$ and $e \in \{1, \dots, D\}$) gives

$$v_\ell^{(1)} \frac{\partial}{\partial s_{ne}} (\tilde{K}_{\ell m} + \tilde{M}_{\ell m} - \lambda_1^h M_{\ell m}) v_m^{(1)} = 0$$

(since $\frac{\partial v_\ell^{(1)}}{\partial s_{ne}}(\tilde{K}_{\ell m} + \tilde{M}_{\ell m} - \lambda_1^h M_{\ell m})v_m^{(1)} = 0$ and $v_\ell^{(1)}(\tilde{K}_{\ell m} + \tilde{M}_{\ell m} - \lambda_1^h M_{\ell m})\frac{\partial v_m^{(1)}}{\partial s_{ne}} = 0$ by (3.5) and the symmetry of the matrices \tilde{K} , \tilde{M} and M). Hence

$$v_\ell^{(1)}\frac{\partial \tilde{K}_{\ell m}}{\partial s_{ne}}v_m^{(1)} + v_\ell^{(1)}\frac{\partial \tilde{M}_{\ell m}}{\partial s_{ne}}v_m^{(1)} - \lambda_1^h v_\ell^{(1)}\frac{\partial M_{\ell m}}{\partial s_{ne}}v_m^{(1)} - \frac{\partial \lambda_1^h}{\partial s_{ne}}v_\ell^{(1)}M_{\ell m}v_m^{(1)} = 0 ,$$

and so, using (3.4),

$$\frac{\partial \lambda_1^h}{\partial s_{ne}} = v_\ell^{(1)}\frac{\partial \tilde{K}_{\ell m}}{\partial s_{ne}}v_m^{(1)} + v_\ell^{(1)}\frac{\partial \tilde{M}_{\ell m}}{\partial s_{ne}}v_m^{(1)} - \lambda_1^h v_\ell^{(1)}\frac{\partial M_{\ell m}}{\partial s_{ne}}v_m^{(1)} , \quad (3.8)$$

for $n \in \{1, \dots, N\}$ and $e \in \{1, \dots, D\}$.

Now

$$\frac{\partial M_{\ell m}}{\partial s_{ne}} = \int_{\Omega} \left(\frac{\partial \alpha_\ell}{\partial s_{ne}} \alpha_m + \alpha_\ell \frac{\partial \alpha_m}{\partial s_{ne}} \right) d\mathbf{x} = - \int_{\Omega} \left(\alpha_n \frac{\partial \alpha_\ell}{\partial x_e} \alpha_m + \alpha_\ell \alpha_n \frac{\partial \alpha_m}{\partial x_e} \right) d\mathbf{x}$$

(by lemma 2.1), and so

$$v_\ell^{(1)}\frac{\partial M_{\ell m}}{\partial s_{ne}}v_m^{(1)} = -2 \int_{\Omega} v_1^h \frac{\partial v_1^h}{\partial x_e} \alpha_n d\mathbf{x} . \quad (3.9)$$

Similarly,

$$v_\ell^{(1)}\frac{\partial \tilde{M}_{\ell m}}{\partial s_{ne}}v_m^{(1)} = -2 \int_{\Omega} q v_1^h \frac{\partial v_1^h}{\partial x_e} \alpha_n d\mathbf{x} . \quad (3.10)$$

Finally

$$\begin{aligned} \frac{\partial \tilde{K}_{\ell m}}{\partial s_{ne}} &= \frac{\partial}{\partial s_{ne}} \int_{\Omega} \frac{\partial \alpha_\ell}{\partial x_i} p_{ij} \frac{\partial \alpha_m}{\partial x_j} d\mathbf{x} \\ &= \sum_{r=1}^E \frac{\partial}{\partial s_{ne}} \int_{\Omega_r} \frac{\partial \alpha_\ell}{\partial x_i} p_{ij} \frac{\partial \alpha_m}{\partial x_j} d\mathbf{x} \\ &\quad (\text{where } \Omega_r \text{ is the } r^{\text{th}} \text{ element of the mesh; } r = 1, \dots, E \text{ say}) \\ &= \sum_{r=1}^{N(n)} \frac{\partial}{\partial s_{ne}} \int_{\Omega_{E(n,r)}} \frac{\partial \alpha_\ell}{\partial x_i} p_{ij} \frac{\partial \alpha_m}{\partial x_j} d\mathbf{x} , \end{aligned}$$

where there are $N(n)$ elements which have node n as a vertex and these have been ordered as $E(n, 1)$ through to $E(n, N(n))$, with $\Omega_{E(n,r)}$ representing each of these elements for r from 1 to $N(n)$. We can now perform a change of variables so that

$$\frac{\partial \tilde{K}_{\ell m}}{\partial s_{ne}} = \sum_{r=1}^{N(n)} \frac{\partial}{\partial s_{ne}} \int_{\Delta} \frac{\partial \alpha_\ell}{\partial x_i} p_{ij} \frac{\partial \alpha_m}{\partial x_j} \left| \frac{d\mathbf{x}}{d\underline{\xi}} \right| d\underline{\xi} , \quad (3.11)$$

where Δ is the standard simplex (with a vertex at the origin and an edge of length 1 in each of the D coordinate directions), and the invertible mapping

$$\mathbf{x}(\underline{\xi}) = \sum_{k=0}^D \underline{x}_k^{(n,r)} \hat{\alpha}_k(\underline{\xi}) \quad (3.12)$$

takes every point in Δ to a unique point in $\Omega_{E(n,r)}$ (where the vertices of $\Omega_{E(n,r)}$ are denoted as the points $\underline{s}_0^{(n,r)}, \dots, \underline{s}_D^{(n,r)}$ and the $\hat{\alpha}_k$ functions are linear basis functions on the standard simplex). By noting that $|\frac{d\underline{x}}{d\underline{\xi}}| = D!A_{E(n,r)}$, where $A_{E(n,r)}(\underline{s})$ is the measure of the simplex $\Omega_{E(n,r)}$, and that

$$\frac{\partial}{\partial s_{ne}} p_{ij}(\underline{x}(\underline{\xi})) = \frac{\partial p_{ij}}{\partial \underline{x}} \cdot \frac{\partial \underline{x}}{\partial s_{ne}} = \frac{\partial p_{ij}}{\partial x_e} \hat{\alpha}_R(\underline{\xi}) \quad (\text{from (3.12)}),$$

where R is the local number such that $\underline{s}_n = \underline{s}_R^{(n,r)}$, we can use (3.11) to deduce that

$$\begin{aligned} \frac{\partial \tilde{K}_{\ell m}}{\partial s_{ne}} &= \sum_{r=1}^{N(n)} \int_{\Delta} \left\{ \frac{\partial \alpha_{\ell}}{\partial x_i} \frac{\partial p_{ij}}{\partial x_e} \frac{\partial \alpha_m}{\partial x_j} \hat{\alpha}_R D!A_{E(n,r)} + p_{ij} \left[\frac{\partial}{\partial s_{ne}} \left(\frac{\partial \alpha_{\ell}}{\partial x_i} \right) \frac{\partial \alpha_m}{\partial x_j} + \frac{\partial \alpha_{\ell}}{\partial x_i} \frac{\partial}{\partial s_{ne}} \left(\frac{\partial \alpha_m}{\partial x_j} \right) \right] D!A_{E(n,r)} \right. \\ &\quad \left. + \frac{\partial \alpha_{\ell}}{\partial x_i} p_{ij} \frac{\partial \alpha_m}{\partial x_j} \frac{\partial}{\partial s_{Re}^{(n,r)}} (D!A_{E(n,r)}) \right\} d\underline{\xi} \\ &= \sum_{r=1}^{N(n)} \int_{\Delta} \left\{ \frac{\partial \alpha_{\ell}}{\partial x_i} \frac{\partial p_{ij}}{\partial x_e} \frac{\partial \alpha_m}{\partial x_j} \alpha_n + p_{ij} \left[\frac{\partial}{\partial x_i} \left(-\alpha_n \frac{\partial \alpha_{\ell}}{\partial x_e} \right) \frac{\partial \alpha_m}{\partial x_j} + \frac{\partial \alpha_{\ell}}{\partial x_i} \frac{\partial}{\partial x_j} \left(-\alpha_n \frac{\partial \alpha_m}{\partial x_e} \right) \right] \right. \\ &\quad \left. + \frac{\partial \alpha_{\ell}}{\partial x_i} p_{ij} \frac{\partial \alpha_m}{\partial x_j} \frac{\partial \alpha_n}{\partial x_e} \right\} D!A_{E(n,r)} d\underline{\xi} \\ &\quad (\text{using lemmas 2.1 and 3.1 and the identity } \hat{\alpha}_R(\underline{\xi}) \equiv \alpha_n(\underline{x}(\underline{\xi}), \underline{s}) \text{ on } \Delta) \\ &= \sum_{r=1}^{N(n)} \int_{\Omega_{E(n,r)}} \left\{ \frac{\partial \alpha_{\ell}}{\partial x_i} \left(\frac{\partial p_{ij}}{\partial x_e} \alpha_n + p_{ij} \frac{\partial \alpha_n}{\partial x_e} \right) \frac{\partial \alpha_m}{\partial x_j} - p_{ij} \left(\frac{\partial \alpha_n}{\partial x_i} \frac{\partial \alpha_{\ell}}{\partial x_e} \frac{\partial \alpha_m}{\partial x_j} + \frac{\partial \alpha_{\ell}}{\partial x_i} \frac{\partial \alpha_n}{\partial x_j} \frac{\partial \alpha_m}{\partial x_e} \right) \right\} d\underline{x} \\ &\quad (\text{since all of the basis functions are linear on each particular element}) \\ &= \int_{\Omega} \left\{ \frac{\partial \alpha_{\ell}}{\partial x_i} \frac{\partial}{\partial x_e} (p_{ij} \alpha_n) \frac{\partial \alpha_m}{\partial x_j} - p_{ij} \left(\frac{\partial \alpha_{\ell}}{\partial x_e} \frac{\partial \alpha_n}{\partial x_i} \frac{\partial \alpha_m}{\partial x_j} + \frac{\partial \alpha_{\ell}}{\partial x_i} \frac{\partial \alpha_n}{\partial x_j} \frac{\partial \alpha_m}{\partial x_e} \right) \right\} d\underline{x}. \end{aligned}$$

Hence

$$\begin{aligned} v_{\ell}^{(1)} \frac{\partial \tilde{K}_{\ell m}}{\partial s_{ne}} v_m^{(1)} &= \int_{\Omega} \frac{\partial v_1^h}{\partial x_i} \frac{\partial}{\partial x_e} (p_{ij} \alpha_n) \frac{\partial v_1^h}{\partial x_j} d\underline{x} - \int_{\Omega} \frac{\partial v_1^h}{\partial x_e} \frac{\partial \alpha_n}{\partial x_i} p_{ij} \frac{\partial v_1^h}{\partial x_j} d\underline{x} - \int_{\Omega} \frac{\partial v_1^h}{\partial x_i} \frac{\partial \alpha_n}{\partial x_j} p_{ij} \frac{\partial v_1^h}{\partial x_e} d\underline{x} \\ &= \int_{\Omega} \frac{\partial v_1^h}{\partial x_i} \frac{\partial}{\partial x_e} (p_{ij} \alpha_n) \frac{\partial v_1^h}{\partial x_j} d\underline{x} - 2 \int_{\Omega} \frac{\partial v_1^h}{\partial x_e} \frac{\partial \alpha_n}{\partial x_i} p_{ij} \frac{\partial v_1^h}{\partial x_j} d\underline{x} \\ &\quad (\text{using the symmetry } p_{ij} = p_{ji}). \end{aligned} \quad (3.13)$$

Thus, combining the results (3.8), (3.9), (3.10) and (3.13) gives the result (3.3), as required. ///

Having established this result about the Galerkin approximation to the fundamental solution mode of (1.3) we now return to our consideration of the Moving Finite Element method for the solution of equation (1.1). First observe that equations (2.11) may be written in the block form

$$\begin{bmatrix} M(\underline{s}) & N^T(\underline{a}, \underline{s}) \\ N(\underline{a}, \underline{s}) & M_2(\underline{a}, \underline{s}) \end{bmatrix} \begin{bmatrix} \dot{\underline{a}} \\ \dot{\underline{s}} \end{bmatrix} = \begin{bmatrix} \underline{g}_1(\underline{a}, \underline{s}) \\ \underline{g}_2(\underline{a}, \underline{s}) \end{bmatrix}, \quad (3.14)$$

corresponding to equations (2.9) and (2.10), where we now use the (revised) notation

$$\underline{a} = (a_1, \dots, a_N)^T$$

$$\begin{aligned}
\underline{s} &= (s_{11}, \dots, s_{1D}; \dots; s_{N1}, \dots, s_{ND})^T \\
\underline{\alpha} &= (\alpha_1, \dots, \alpha_N)^T \\
\underline{\beta} &= (\beta_{11}, \dots, \beta_{1D}; \dots; \beta_{N1}, \dots, \beta_{ND})^T \\
M(\underline{s}) &= \langle \underline{\alpha}, \underline{\alpha}^T \rangle \quad (\text{as already defined}) \\
N(\underline{a}, \underline{s}) &= \langle \underline{\alpha}, \underline{\beta}^T \rangle \\
M_2(\underline{a}, \underline{s}) &= \langle \underline{\beta}, \underline{\beta}^T \rangle .
\end{aligned}$$

Hence,

$$M(\underline{s})\dot{\underline{a}} + N^T(\underline{a}, \underline{s})\dot{\underline{s}} = \underline{g}_1(\underline{a}, \underline{s}), \quad (3.15)$$

and so

$$(M_2(\underline{a}, \underline{s}) - N(\underline{a}, \underline{s})M^{-1}(\underline{s})N^T(\underline{a}, \underline{s}))\dot{\underline{s}} = \underline{g}_2(\underline{a}, \underline{s}) - N(\underline{a}, \underline{s})M^{-1}(\underline{s})\underline{g}_1(\underline{a}, \underline{s}) \quad (3.16)$$

gives an equation for the motion of the node points of the mesh.

Theorem 3.3 *Suppose there exists a solution of the Moving Finite Element equations (3.14) for which $\underline{s} = \underline{s}^*$ for all t (i.e. $\dot{\underline{s}} = \underline{0}$). Then*

$$\underline{a} = ke^{-\lambda_1^h(\underline{s}^*)t}\underline{v}^{(1)}(\underline{s}^*), \quad \underline{s} = \underline{s}^*$$

must also be such a solution, where $\lambda_1^h(\underline{s}^)$ is the smallest eigenvalue of $M^{-1}(\underline{s}^*)(\tilde{K}(\underline{s}^*) + \tilde{M}(\underline{s}^*))$ and $v_1^h(\underline{x}, \underline{s}^*) = \sum_{m=1}^N v_m^{(1)}(\underline{s}^*)\alpha_m(\underline{x}, \underline{s}^*)$ is a corresponding normalized eigenfunction. Moreover, for this solution*

$$\frac{\partial \lambda_1^h}{\partial \underline{s}}(\underline{s}^*) = \underline{0}$$

and, provided that $v_1^h(\underline{x}, \underline{s}^)$ is not degenerate, if this MFE solution is stable, the Hessian matrix $\frac{\partial}{\partial \underline{s}}(\frac{\partial \lambda_1^h}{\partial \underline{s}})$ will be positive definite when evaluated at $\underline{s} = \underline{s}^*$ and so $\lambda_1^h(\underline{s}^*)$ is a local minimum of $\lambda_1^h(\underline{s})$.*

Proof From (2.9) and (3.15) it follows that when $\underline{s} = \underline{s}^*$ and $\dot{\underline{s}} = \underline{0}$

$$M(\underline{s}^*)\dot{\underline{a}} = \underline{g}_1(\underline{a}, \underline{s}^*) = -(\tilde{K}(\underline{s}^*) + \tilde{M}(\underline{s}^*))\underline{a} \quad (3.17)$$

and so the solution

$$\underline{a} = ke^{-\lambda_1^h(\underline{s}^*)t}\underline{v}^{(1)}(\underline{s}^*) \quad (= \underline{a}^*(\underline{s}^*) \text{ say}),$$

is clearly admitted. Now observe that with an arbitrary choice of \underline{s} and with

$$\underline{a} = \underline{a}^*(\underline{s}) = ke^{-\lambda_1^h(\underline{s})t}\underline{v}^{(1)}(\underline{s}) \quad (3.18)$$

(i.e. $u^h(\underline{x}, t) = ke^{-\lambda_1^h(\underline{s})t}v_1^h(\underline{x}, \underline{s})$), we have, using (3.17) and (3.18),

$$\begin{aligned} N(\underline{a}^*, \underline{s})M^{-1}(\underline{s})\underline{g}_1(\underline{a}^*, \underline{s}) &= -N(\underline{a}^*, \underline{s})M^{-1}(\underline{s})(\tilde{K}(\underline{s}) + \tilde{M}(\underline{s}))ke^{-\lambda_1^h(\underline{s})t}\underline{v}^{(1)}(\underline{s}) \\ &= -\lambda_1^h(\underline{s})N(\underline{a}^*, \underline{s})ke^{-\lambda_1^h(\underline{s})t}\underline{v}^{(1)}(\underline{s}), \end{aligned}$$

which has the components

$$\lambda_1^h k^2 e^{-2\lambda_1^h t} \int_{\Omega} v_1^h \alpha_n \frac{\partial v_1^h}{\partial x_e} d\underline{x} \quad (3.19)$$

for $n = 1, \dots, N$ and $e = 1, \dots, D$. Also, from (2.10), we see that $\underline{g}_2(\underline{a}^*, \underline{s})$ has the components

$$\int_{\Omega} qk^2 e^{-2\lambda_1^h t} v_1^h \alpha_n \frac{\partial v_1^h}{\partial x_e} d\underline{x} - \frac{1}{2} \int_{\Omega} k^2 e^{-2\lambda_1^h t} \frac{\partial v_1^h}{\partial x_i} \frac{\partial v_1^h}{\partial x_j} \frac{\partial}{\partial x_e} (\alpha_n p_{ij}) d\underline{x} + \int_{\Omega} p_{ij} k^2 e^{-2\lambda_1^h t} \frac{\partial v_1^h}{\partial x_j} \frac{\partial \alpha_n}{\partial x_i} \frac{\partial v_1^h}{\partial x_e} d\underline{x}, \quad (3.20)$$

for $n = 1, \dots, N$ and $e = 1, \dots, D$, where the results of lemma 2.1 have been used where necessary to obtain (3.20). Combining these last two expressions, (3.19) and (3.20), with lemma 3.2 leads to the following equality:

$$\underline{g}_2(\underline{a}^*(\underline{s}), \underline{s}) - N(\underline{a}^*(\underline{s}), \underline{s})M^{-1}(\underline{s})\underline{g}_1(\underline{a}^*(\underline{s}), \underline{s}) = -\frac{1}{2}k^2 e^{-2\lambda_1^h(\underline{s})t} \frac{\partial \lambda_1^h}{\partial \underline{s}}(\underline{s}). \quad (3.21)$$

Now when $\underline{s} = \underline{s}^*$ it follows that $\underline{a} = \underline{a}^*(\underline{s}^*) = ke^{-\lambda_1^h(\underline{s}^*)t}\underline{v}^{(1)}(\underline{s}^*)$ satisfies (3.15) and (3.16) implies that

$$\underline{g}_2(\underline{a}^*(\underline{s}^*), \underline{s}^*) - N(\underline{a}^*(\underline{s}^*), \underline{s}^*)M^{-1}(\underline{s}^*)\underline{g}_1(\underline{a}^*(\underline{s}^*), \underline{s}^*) = \underline{0},$$

hence by (3.21),

$$\frac{\partial \lambda_1^h}{\partial \underline{s}}(\underline{s}^*) = \underline{0}, \quad (3.22)$$

as claimed.

For the final part of the proof we need to linearize (3.16) about the known solution $\underline{s} = \underline{s}^*$ and $\underline{a} = \underline{a}^*(\underline{s}^*)$ with respect to perturbations in \underline{s} , so as to obtain

$$\begin{aligned} (M_2(\underline{a}^*(\underline{s}^*), \underline{s}^*) - N(\underline{a}^*(\underline{s}^*), \underline{s}^*)M^{-1}(\underline{s}^*)N^T(\underline{a}^*(\underline{s}^*), \underline{s}^*))\dot{\underline{s}} \\ = \left[\frac{\partial}{\partial \underline{s}} \{ \underline{g}_2(\underline{a}^*(\underline{s}), \underline{s}) - N(\underline{a}^*(\underline{s}), \underline{s})M^{-1}(\underline{s})\underline{g}_1(\underline{a}^*(\underline{s}), \underline{s}) \} \Big|_{(\underline{s}=\underline{s}^*)} \right] \dot{\underline{s}} \\ = \left[\frac{\partial}{\partial \underline{s}} \left\{ -\frac{1}{2}k^2 e^{-2\lambda_1^h(\underline{s})t} \frac{\partial \lambda_1^h}{\partial \underline{s}}(\underline{s}) \right\} \Big|_{(\underline{s}=\underline{s}^*)} \right] \dot{\underline{s}} \end{aligned}$$

(using (3.21)). Hence if the solution with $\underline{s} = \underline{s}^*$ is linearly stable, the matrix

$$(M_2 - NM^{-1}N^T)^{-1} \frac{\partial}{\partial \underline{s}} \left\{ -\frac{1}{2}k^2 e^{-2\lambda_1^h t} \frac{\partial \lambda_1^h}{\partial \underline{s}} \right\}$$

must have no positive eigenvalues when evaluated at $\underline{s} = \underline{s}^*$. However

$$\begin{bmatrix} M & 0 \\ 0 & M_2 - NM^{-1}N^T \end{bmatrix} = \begin{bmatrix} I & 0 \\ -NM^{-1} & I \end{bmatrix} \begin{bmatrix} M & N^T \\ N & M_2 \end{bmatrix} \begin{bmatrix} I & -(NM^{-1})^T \\ 0 & I \end{bmatrix}$$

and so if the MFE mass matrix in (3.14) is positive definite so is the matrix $M_2 - NM^{-1}N^T$. Given that the solution $v_1^h(\underline{s}^*)$ is not degenerate (see lemma 2.2) then this is indeed the case. Hence, if the solution with $\underline{s} = \underline{s}^*$ is stable

$$\frac{\partial}{\partial \underline{s}} \left\{ -\frac{1}{2} k^2 e^{-2\lambda_1^h t} \frac{\partial \lambda_1^h}{\partial \underline{s}} \right\} \Big|_{(\underline{s}=\underline{s}^*)}$$

must be negative definite. Thus, using (3.22), the Hessian of $\lambda_1^h(\underline{s})$ evaluated at $\underline{s} = \underline{s}^*$ is shown to be positive definite as required. ///

The above theorem reveals an important property of any stationary meshes that may be produced by the Moving Finite Element method and we will see in the next section that typical MFE solutions do indeed have such meshes as stable attractors. However it is not sufficient merely to show that such solutions minimize the value of $\lambda_1^h(\underline{s})$ (and therefore the asymptotic rate of decay of solutions to (1.1) for large times): we would really like to demonstrate that the error, $|\lambda_1 - \lambda_1^h(\underline{s})|$, is minimized. Fortunately this result follows easily from the above theorem.

Corollary 3.4 *If the Moving Finite Element method is applied to (1.1) and yields a solution which tends to a fixed mesh, then this mesh is optimal in the sense that*

- (i) *the Galerkin solution to (1.3) on this mesh gives an optimal approximation to the fundamental eigenvalue, λ_1 ,*
- (ii) *the rate of decay of the MFE solution to (1.1) is optimal for large times.*

Proof It is sufficient to derive an expression of the form (3.2) from the above theorem. However this is straightforward once we observe (see [17] for example) that

$$\lambda_1 = \min_{v \in H_0^1(\Omega)} R(v) \quad \text{and} \quad \lambda_1^h(\underline{s}) = \min_{v^h \in S_0^h(\underline{s})} R(v^h),$$

where $R(v)$ is the Rayleigh quotient defined by (3.1). Because $S_0^h(\underline{s}) \subset H_0^1(\Omega)$ this shows that $\lambda_1 \leq \lambda_1^h(\underline{s})$ for all meshes \underline{s} and so if $\lambda_1^h(\underline{s}^*) \leq \lambda_1^h(\underline{s})$, as demonstrated by theorem 3.3, (3.2) follows immediately. ///

4 Some Numerical Examples

In this section we illustrate the main result of the paper with the aid of two numerical studies; both for the two-dimensional case, $D = 2$ (see [6] for a number of one-dimensional experiments). We emphasize that these experiments are for the purpose of verification only and we do not suggest that the MFE algorithm, in the form analyzed here, is the most practical form of adaptivity for these linear examples.

The test problems that we consider are

$$\frac{\partial u}{\partial t} = \nabla^2 u; \quad \Omega = (0, 1) \times (0, 1); \quad u|_{\partial\Omega} = 0, \quad (4.1)$$

and

$$\frac{\partial u}{\partial t} = \frac{1}{\pi^2} \nabla^2 u - (e^{\pi x_1} + e^{\pi x_2})u; \quad \Omega = (0, 1) \times (0, 1); \quad u|_{\partial\Omega} = 0. \quad (4.2)$$

In the first case we are able to compare our numerical solutions with the known analytic solution and in the second case an accurate estimate of the dominant eigenvalue is known (e.g. [16, appendix A]).

Because we know the exact analytic solution to the first problem for arbitrary initial data we can deduce the asymptotic behaviour of this solution for large times, t :

$$u(\underline{x}, t) \sim e^{-2\pi^2 t} \sin(\pi x_1) \sin(\pi x_2) \quad \text{as } t \rightarrow \infty.$$

Hence the dominant eigenvalue, λ_1 , is equal to $2\pi^2$. If we solve this problem numerically using the Moving Finite Element method, starting on a regular mesh containing 64 elements and 41 nodes, of which 25 are interior to the domain, then the MFE problem has 75 degrees of freedom. Figure 1 shows the evolution of this mesh for a solution with initial data chosen to be the piecewise linear interpolant of $\sin(\pi x_1) \sin(\pi x_2)$. The meshes shown (from top left to bottom right) are the solution meshes calculated at times 0.0, 0.01, 0.02 and 1.0, by which time the mesh is stationary. Table 1 lists the positions of the node points in this stationary mesh which, according to the results of the previous section should be an optimal mesh for approximating the diffusion rate of the asymptotic solution. To verify that this is indeed the case we make use of the NAG library ([14]) optimization routine E04JAF and the symmetric generalized eigenvalue routine F02ADF. With the aid of these subroutines it is easy to demonstrate that this stationary mesh is indeed a local minimizer of $\lambda_1^h(\underline{s})$, the dominant eigenvalue of the matrix $M^{-1}(\underline{s})\tilde{K}(\underline{s})$, over all local variations in \underline{s} . (Note that for this example $p_{ij} = \delta_{ij}$ in the definition of \tilde{K} and $q = 0$ in the definition of \tilde{M} , which means that \tilde{M} is zero: see (3.6).) It is also possible to verify that the dominant eigenvalue of $M^{-1}(\underline{s})\tilde{K}(\underline{s})$, corresponding to this optimal mesh, and the large-time diffusion rate of the MFE solution, also on this mesh, are identical, taking the value of 20.393364 (to 6 decimal places).

We now move on to the numerical solution of the second problem, (4.2). First however, observe that if we apply separation of variables to this equation, so as to represent $u(\underline{x}, t)$ by $X_1(x_1)X_2(x_2)T(t)$ say, we reduce the problem to that of solving the o.d.e.'s

$$\frac{-1}{\pi^2} X_i''(x_i) + e^{\pi x_i} X_i(x_i) = \lambda X_i(x_i); \quad X_i(0) = X_i(1) = 0,$$

for $i = 1, 2$. These problems are equivalent to the Paine problem, considered in [15], whose eigenvalues are tabulated in [16, appendix A]. In particular, the dominant eigenvalue is 4.89666938 (to 8 decimal

places) and hence the asymptotic diffusion rate of the solution to the two-dimensional problem, (4.2), is equal to twice this value: 9.97333876 (to 8 decimal places).

Again we may solve the problem using the MFE method on a grid with 64 elements and 41 nodes, starting with the same uniform mesh and the same initial data as for the previous example. Figure 2 shows the evolution of this finite element mesh, at times 0.1, 0.2 and 10.0 (bottom right), by which time the mesh is stationary. The final column of table 1 lists the positions of the nodes in this stationary mesh. Again it is possible to use the NAG library routines to verify that this mesh is also a local minimizer of $\lambda_1^h(\underline{s})$, where now $\lambda_1^h(\underline{s})$ is the dominant eigenvalue of $M^{-1}(\underline{s})(\tilde{K}(\underline{s}) + \tilde{M}(\underline{s}))$ with $p_{ij} = \frac{1}{\pi^2} \delta_{ij}$ and $q = e^{\pi x_1} + e^{\pi x_2}$ in the definitions of \tilde{K} and \tilde{M} , (3.6).

In both of the above cases we have demonstrated that when the MFE solution tends to a stationary mesh we get an optimal eigenvalue estimate as predicted. Unfortunately however it is not always the case that the mesh evolves to a stationary position without difficulty. Consider, for example, solving the first of the problems again, this time using the regular initial mesh in figure 3 which contains 256 elements and 145 nodes (again we take the interpolant of $\sin(\pi x_1) \sin(\pi x_2)$ as the initial data.) As the solution evolves, the nodes move in such a way that some of them run into each other in finite time, causing some elements to shrink to zero area, as seen in the second mesh of figure 3 (corresponding to the time 0.0006). This is one of the main drawbacks of the MFE method as analyzed here, however more practical implementations are possible – using penalty functions to keep nodes apart (as in [12] for example); or else removing nodes from the mesh altogether when appropriate (as in [10]).

To finish this section we note that the reason for the difficulty with obtaining a stationary mesh in the last example is that the initial mesh was not close enough to the optimal mesh. To see this, we can consider the topologically equivalent initial mesh shown in figure 4 (left) which is obtained by performing a uniform h -refinement of the stationary mesh in figure 1. We now see that there does exist an MFE solution with a stationary 145 node mesh which can be found provided the initial mesh is sufficiently close to it. This final mesh also yields an optimal approximation to the eigenvalue $2\pi^2$.

5 Discussion

In this paper we have shown that for the linear parabolic equation (1.1) the Moving Finite Element method is capable of producing an optimal mesh in the sense that the large-time solution will decay at the best possible rate compared to the exact asymptotic solution. This corresponds to obtaining the optimal mesh on which to approximate the smallest eigenvalue for equation (1.3). Although the theory and numerical examples have been presented here only for the special case of

homogeneous Dirichlet boundary conditions of the form (1.2), the results are not restricted just to this special case, with extensions to fixed Neumann boundaries being quite straightforward for example. Also, it is worth noting that the results of this paper complement those presented in [7] which deals with equation (1.1) but with a positive source term present on the right-hand-side. In that paper it is shown that the MFE method can give optimal steady-state solutions, and here we have made the first step towards understanding the temporal properties of the method for parabolic problems.

There are a number of limitations to the theory presented here which are yet to be addressed. For example, no account is taken of the fact that numerical quadrature is used in the practical implementation of the MFE method. Also, it would be useful to extend the results here to take into account the use of penalty functions of the sort proposed by Miller ([12]), which are designed to prevent elements from shrinking to zero as can be observed in figure 3. The most important extensions however will be to deal with wider problem classes, such as nonlinear parabolic equations or systems, and to better understand the behaviour of the mesh during the initial transients, rather than just for large times.

A final observation that is worth making is that whilst the optimal solutions computed in section 4 have been calculated extremely accurately, to 8 decimal places, from a practical point of view there is no need to require the mesh locations to such high accuracy (especially if numerical quadrature is being used). The node points evolve very quickly to within a very small distance of their final position and so it is likely that for most purposes the conventional Galerkin solution will give a perfectly satisfactory “pseudo-optimal” solution if it is employed after taking a relatively small number of time-steps with the MFE algorithm (which is a lot more expensive than the Galerkin algorithm) in order to evolve the mesh to an almost optimal state.

References

- [1] M J Baines (1985). *Locally Adaptive Moving Finite Elements*. Numerical Methods for Fluid Dynamics II (eds. K W Morton & M J Baines), Oxford University Press.
- [2] M J Baines (1994). *Moving Finite Elements*. Oxford University Press.
- [3] M J Baines and A J Wathen (1986). *Moving Finite Element Modelling of Compressible Flow*. Applied Num. Maths., 2, 495–514.
- [4] M J Baines and A J Wathen (1988). *Moving Finite Element Methods for Evolutionary Problems. I. Theory*. J. of Comp. Phys., 79, 245–269.

- [5] R J Gelinias, S K Doss and K Miller (1981). *The Moving Finite Element Method: Application to General Partial Differential Equations with Multiple Large Gradients*. J. of Comp. Phys., 40, 202–249.
- [6] P K Jimack (1992) *On Steady and Large Time Solutions of the Semi-Discrete Moving Finite Element Equations for One-Dimensional Diffusion Equations*. IMA J. Num. Anal., 12, 545–564.
- [7] P K Jimack (1993) *A Best Approximation Property of the Moving Finite Element Method*. To appear, SIAM J. Num. Anal.
- [8] P K Jimack and A J Wathen(1991) *Temporal Derivatives in the Finite Element Method on Continuously Deforming Grids*. SIAM J. Num. Anal., 28, 990–1003.
- [9] I W Johnson, A J Wathen and M J Baines (1988). *Moving Finite Element Methods for Evolutionary Problems. II. Applications*. J. of Comp. Phys., 79, 270–297.
- [10] A Kuprat (1992). *Creation and Annihilation of Nodes for the Moving Finite Element Method*. Ph.D. Thesis, University of California at Berkeley. Unpublished.
- [11] K Miller and R Miller (1981). *Moving Finite Elements, Part I*. SIAM J. Num. Anal., 18, 1019–1032.
- [12] K Miller (1981). *Moving Finite Elements, Part II*. SIAM J. Num. Anal., 18, 1033–1057.
- [13] A C Mueller and G F Carey (1985). *Continuously Deforming Finite Elements*. Int. J. Num. Meth. Eng., 21, 2099–2126.
- [14] Numerical Algorithms Group Limited (1993) *The NAG Fortran Library Manual – Mark 14*.
- [15] J W Paine, F R de Hoog and R S Anderson (1981). *On the Correction of Finite Difference Eigenvalue Approximations for Sturm-Liouville Systems*. Computing, 26, 123–139.
- [16] J D Pryce (1993). *Numerical Solution of Sturm-Liouville Problems*. Clarendon Press, Oxford, UK.
- [17] G Strang and G J Fix (1973). *An Analysis of the Finite Element Method*. Prentice-Hall
- [18] A J Wathen (1986) *Mesh Independent Spectra in the Moving Finite Element Equations*. SIAM J. Num. Anal., 23, 797–814.
- [19] A J Wathen and M J Baines (1985). *On the Structure of the Moving Finite Element Equations*. IMA J. Num. Anal., 5, 161–182.

i	Initial \underline{s}_i^T	\underline{s}_i^T (1st problem)	\underline{s}_i^T (2nd problem)
1	(0.50000000, 0.50000000)	(0.50000000, 0.50000000)	(0.29874693, 0.29874693)
2	(0.25000000, 0.75000000)	(0.38129616, 0.61870384)	(0.15145258, 0.68819694)
3	(0.25000000, 0.25000000)	(0.38129616, 0.38129616)	(0.22981733, 0.22981733)
4	(0.75000000, 0.25000000)	(0.61870384, 0.38129616)	(0.68819694, 0.15145258)
5	(0.75000000, 0.75000000)	(0.61870384, 0.61870384)	(0.59610266, 0.59610266)
6	(0.25000000, 0.50000000)	(0.36335788, 0.50000000)	(0.21765127, 0.32542608)
7	(0.37500000, 0.62500000)	(0.45237639, 0.54762361)	(0.26167747, 0.34059459)
8	(0.37500000, 0.37500000)	(0.45237639, 0.45237639)	(0.27152474, 0.27152474)
9	(0.12500000, 0.87500000)	(0.10445583, 0.89554417)	(0.09722501, 0.81370597)
10	(0.12500000, 0.62500000)	(0.25352857, 0.56134688)	(0.05806621, 0.60347872)
11	(0.12500000, 0.37500000)	(0.25352857, 0.43865312)	(0.15363905, 0.28797883)
12	(0.12500000, 0.12500000)	(0.10445583, 0.10445583)	(0.05511770, 0.05511770)
13	(0.50000000, 0.25000000)	(0.50000000, 0.36335788)	(0.32542608, 0.21765127)
14	(0.62500000, 0.37500000)	(0.54762361, 0.45237639)	(0.34059459, 0.26167747)
15	(0.37500000, 0.12500000)	(0.43865312, 0.25352857)	(0.28797883, 0.15363905)
16	(0.62500000, 0.12500000)	(0.56134688, 0.25352857)	(0.60347872, 0.05806621)
17	(0.87500000, 0.12500000)	(0.89554417, 0.10445583)	(0.81370597, 0.09722501)
18	(0.75000000, 0.50000000)	(0.63664212, 0.50000000)	(0.36673163, 0.29884697)
19	(0.62500000, 0.62500000)	(0.54762361, 0.54762361)	(0.32667015, 0.32667015)
20	(0.50000000, 0.75000000)	(0.50000000, 0.63664212)	(0.29884697, 0.36673163)
21	(0.87500000, 0.37500000)	(0.74647143, 0.43865312)	(0.75382175, 0.30446709)
22	(0.87500000, 0.62500000)	(0.74647143, 0.56134688)	(0.73654512, 0.43798158)
23	(0.87500000, 0.87500000)	(0.89554417, 0.89554417)	(0.71755576, 0.71755576)
24	(0.62500000, 0.87500000)	(0.56134688, 0.74647143)	(0.43798158, 0.73654512)
25	(0.37500000, 0.87500000)	(0.43865312, 0.74647143)	(0.30446709, 0.75382175)

Table 1: The positions of the 25 free node points in the stationary mesh obtained from the MFE solutions of the first two test problems (along with their starting positions in the initial regular mesh).

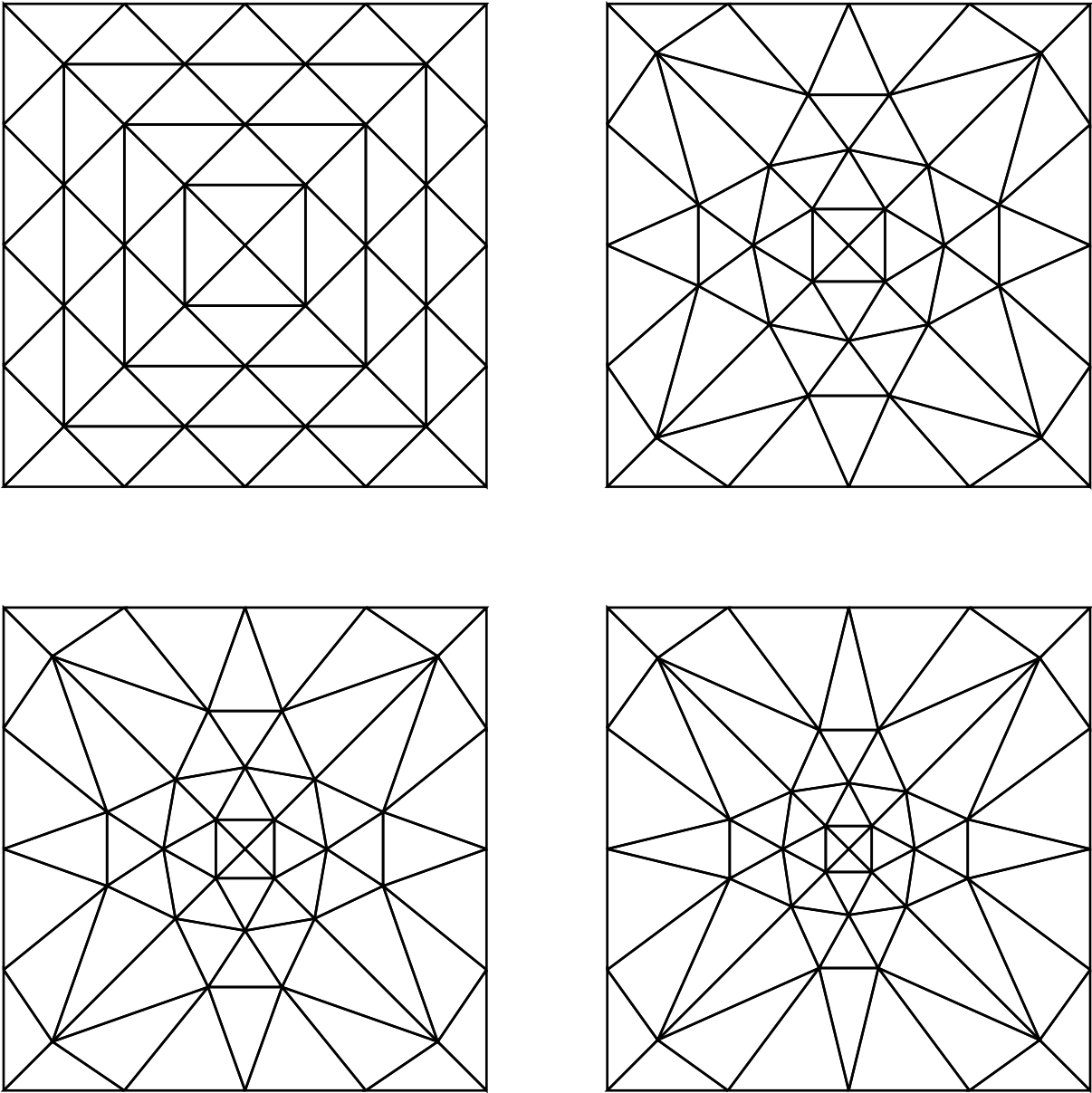


Figure 1: Evolution of an MFE solution mesh when solving the first test problem.

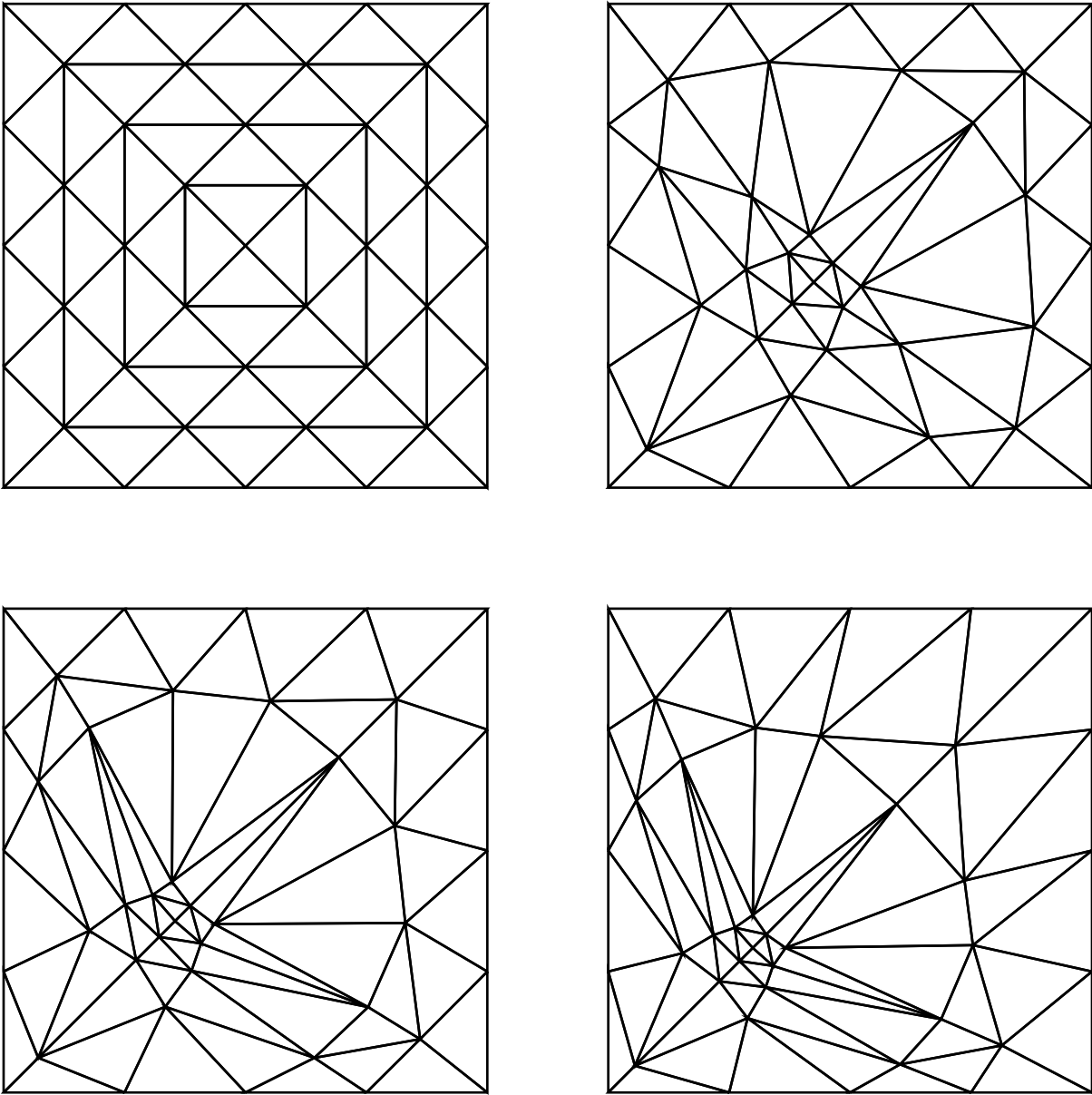


Figure 2: Evolution of an MFE solution mesh when solving the second test problem.

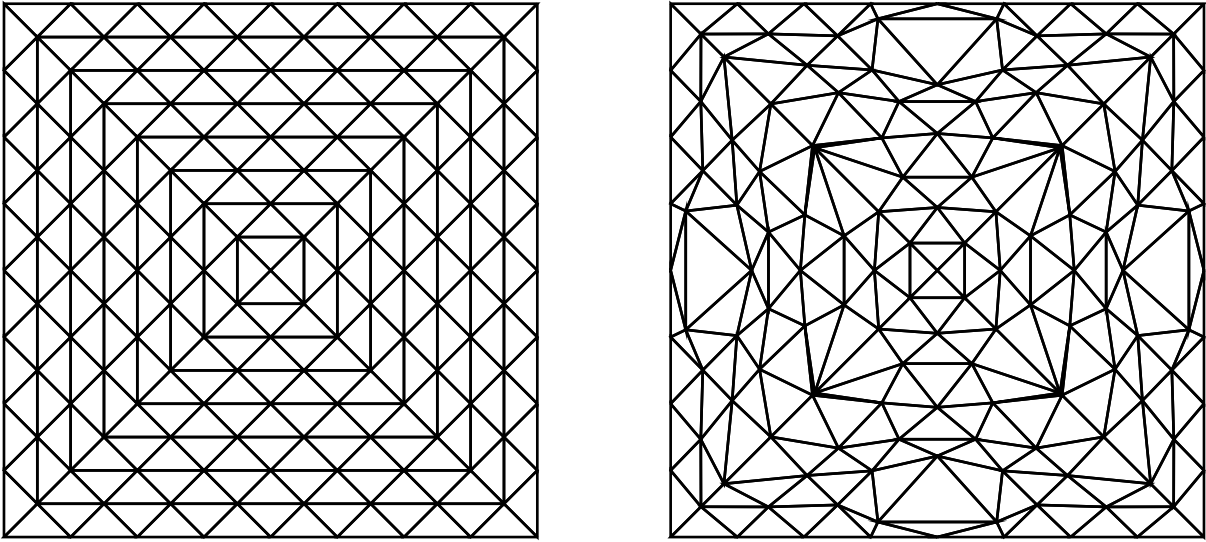


Figure 3: An MFE solution mesh with eight elements shrinking to zero area.

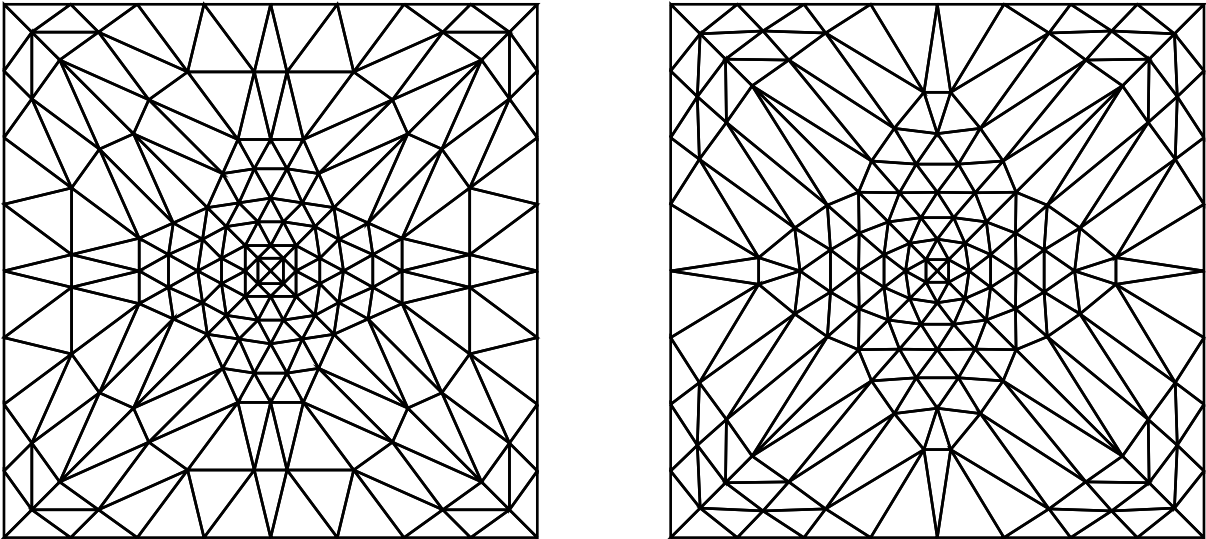


Figure 4: A finer MFE solution mesh for solving the first problem.